Tidal Effects on Seabird-Bathymetry Associations and Physical Oceanography in the San Juan Channel

Emma L. Schlatter[1]

Pelagic Ecosystem Function Research Apprenticeship

Fall 2013

[1] Friday Harbor Laboratories, University of Washington, Friday Harbor, WA 98250

Contact information:

emmaschlatter@gmail.com

Key words: Tidal phase, tidal currents, tidal exchange, ebb-flood, spring-neap, water density, fine-scale sampling, San Juan Channel, Cattle Pass, Griffin Bay, bathymetry, shallow sill, tidal coupling, seabird abundance, seabird distribution

Part I: Tides and physical oceanography in the southern San Juan Channel

ABSTRACT

In the southern San Juan Channel, flood tides bring an influx of cold, saline oceanic water, while warmer, fresher water flows out of the channel on ebb tides. Variation in tidal conditions thus has important effects on the physical properties of the water in the channel. The objective of this study was to measure these effects on both slack-flood and spring-neap scales of tidal variation. To accomplish this, measurements of physical water properties were taken repeatedly in the same location over the course of a flood tide on four consecutive days. Water density was found to increase as the flood tide progressed within each day, and also as tidal condition changed from neap to spring over the course of the four days. Data taken under similar tidal and seasonal conditions in 2012 did not show the same strong relationship, but given unusually cold water temperatures present in the channel in 2012, this is not inconsistent with the previously stated model of how tidal input affects physical water properties.

INTRODUCTION

Physical oceanography is crucial to interpretation of other observations in a pelagic environment, from ocean chemistry to biology at all trophic levels. Temperature, salinity, density, and their distribution in the water column affect ecosystem function in many ways. Because temperature and salinity affect the saturation state of oxygen in seawater, a meaningful interpretation of oxygen levels as an indicator of biological activity requires information about temperature and salinity (Williams 2012). At higher trophic levels, stratification in the water column controls the availability of prey to surface-feeding predators and is therefore important background to a study of predator distribution.

In the estuarine system of the San Juan Channel, physical oceanographic properties undergo constant change due to strong tidal forcing. The mixed semidiurnal tidal cycle characteristic of the western coast of North America incorporates two scales of

variation: ebb-flood and spring-neap. Tidal height and current speed vary on the ebb-flood scale, with two ebbs and two floods each day. In the southern San Juan Channel, flood tides bring cool, saline oceanic water from the Strait of Juan de Fuca in the south, while ebb tides transport warmer, fresher water from the Strait of Georgia in the north. The relative strength and degree of mixing of these two signals in the channel is influenced by tidal phase and intensity. Daily exchange and the difference between the two cycles in a day vary according to the biweekly spring-neap cycle.

Previous work in the southern San Juan Channel has investigated the effects of both scales of tidal forcing on physical oceanography. Tidal exchange, greater on spring tides than neap, has been shown to increase vertical mixing (Tolkin 2007, Harmann 2008) and also affects pycnocline depth and width (Bernard 2010, Thomas 2011). Eisenlord (2012) demonstrated that tidal forcing on the ebb-flood scale affects near-surface water properties. Her findings suggested an increase in density over the course of a flood tide, but did not quantify this effect.

The goal of the present study was to examine tidal sources of variation in physical oceanography in the southern San Juan Channel. The study was designed to be consistent with the methodology of Eisenlord (2012) to facilitate comparison between datasets. Specific objectives were as follows:

- Characterize variation in near-surface physical oceanography at a site near Griffin Bay over four days in October 2013
- Relate variation in physical oceanography to tidal conditions on ebb-flood and spring-neap scales

- Compare effects in 2012 and 2013 of tidal forcing on near-surface physical oceanography at Griffin Bay

METHODS

Physical Oceanography Measurements

A Seabird Electronics, Inc., model SEACAT SBE-19 CTD equipped with temperature, conductivity, and depth sensors was deployed from a small boat, soaked at the surface for 3 minutes, lowered by hand to a depth of 20 meters, and retrieved. This process was repeated at 30-minute intervals from high low tide through peak flood (a span of 4.5 to 5 hours) each day from 16 to 19 October, 2013. Measurements were taken at 48.4708°N, 122.9598°W (Figure 1). Start times were based on slack low tide predictions for San Juan Channel, South Entrance, accessed through Mr. Tides software. Sampling times were chosen to match tidal conditions from 2012 as closely as possible (Figure 2).

Data Processing and Analysis

The CTD data were processed using manufacturer-provided software. Data were imported using the SeaTerm program and processed using SBE Data Processing software, then imported into Microsoft Excel spreadsheets for plotting. Contour plots and regression analyses were created using SigmaPlot. Analysis was performed on data from 36 CTD casts in 2013 (9 casts per day over 4 days) and 27 casts in 2012 (obtained from Eisenlord 2012).

Two values associated with tidal conditions were calculated for each cast. *Time since slack low* was defined as the difference between cast time and time of slack low tide, as obtained from Mr. Tides software current velocity prediction for San Juan

Channel, South Entrance. *Previous tidal range* was a measure of prior tidal exchange defined as the difference between maximum and minimum tidal height in the 18 hours preceding sampling, based on NOAA's tidal height predictions for Friday Harbor station (http://tidesandcurrents.noaa.gov/noaatidepredictions/NOAATidesFacade.jsp?Stationid=9449880). At all four *previous tidal range* values, measurements were taken for each *time since slack low* value, so the two variables were uncorrellated.

Temperature and salinity values collected by standard methods from CTD casts during weekly cruises on the R/V Centennial (see Thompson 2013) were used to indicate typical near-surface water properties in the channel during October 2012 and 2013. Data used in these calculations were collected from the top 20m of water at stations at the north and south ends of the channel (stations N and S; see Figure 1). Tidal conditions for each cruise used in these calculations were defined based on NOAA tidal current predictions for Turn Rock (http://tides.mobilegeographics.com/locations/6623.html), and are displayed in Table 1.

RESULTS

Temperature and Salinity Conditions: Griffin Bay vs. Centennial Stations N and S

The October 2013 temperature and salinity conditions from the Griffin Bay site closely match those at the R/V Centennial station S, but fall outside the norm for station N (Figure 3b). Temperature measurements at the Griffin Bay site over the four days of sampling in 2013 varied from 9.80°C to 10.35°C, while salinity ranged from 30.11 PSU to 30.88 PSU. These values span approximately one standard deviation from mean values at station S in both temperature and salinity.

Conditions at Griffin Bay did not closely match stations N or S in 2012 (Figure 3a). Over the four days of sampling at Griffin Bay, water properties were measured from 9.24°C to 9.37°C and 30.65 PSU to 31.10 PSU. In contrast to 2013, the range of data collected at Griffin Bay was much narrower than the range of typical Centennial values for station S. Salinity at Griffin Bay was around typical mean value for station S, and temperature fell at the low end of typical range for both stations.

Overall, R/V Centennial data indicate that water was colder and more saline in 2012 than 2013 (Figure 4). The average temperature at station S was 0.63°C lower in 2012 than 2013, while average salinity was 0.45 PSU higher in 2012. Station N averages were 0.61°C colder and 0.72 PSU saltier in 2012. Temperature was also more variable in 2012, particularly at Station N, where the standard deviation of temperature was 0.49 in 2012 and 0.15 in 2013.

Depth Patterns

At most sampling times, water properties at Griffin Bay in 2013 did not vary substantially with depth. Of the 36 CTD casts measuring water at depths of 1.5m to 20m, only five had a range in density greater than 0.15 σ_T. By comparison, density over the entire sampling period had a range of 0.66 σ_T.

The highest variation in density was found near the time of peak flood: all samples with density range greater than 0.15 σ_T were taken 3 to 4.5 hours after slack low tide. In many of these samples, denser water was present at shallower depths than less dense water. This can be seen in density contour plots (Figure 5) by areas of cool colors (representing greater density) above warmer ones.

Temporal Patterns in 2013

In 2013, mean water density from depths of 1.5m to 12.5m at the Griffin Bay site increased as the incoming tide progressed from slack low to fast flood. This pattern was observed on each of the four sampling days in 2013. Based on a linear regression, 29% of the variation in water density over the four days of sampling can be explained by time since slack low (Figure 6c). The range in density from slack low to fast flood was similar on all four days: 16 October had the greatest range, 0.4 σ_T, while 19 October had the smallest, 0.3 σ_T.

Despite the overall pattern of increase in mean water density with time, on the 17th, 18th and 19th a brief decrease in density was observed following the fast flood (Figure 6a). In each case, density decreased to slightly above the slack low value for that day. On the 17th and 19th, this dip was followed by an increase, while on the 18th the decrease continued for the remainder of the day's sampling.

Mean water density increased from day to day as the tide transitioned from neap to spring. The average density for all samples in a day increased from 23.34σ_T on October 16 to 23.53σ_T on October 19. A linear regression showed that previous tidal range (which varies according to the change from neap tide to spring) accounts for 33% of the observed variation in water density (Figure 7b).

2012-2013 Comparison

Physical water properties at the Griffin Bay site in 2012 differed from 2013 in several ways. Water was much denser in 2012 than in 2013. The minimum density (averaged over depths of 1.5m to 12.5m) of a CTD cast in 2012 was 23.73 σ_T, slightly greater than the 2013 maximum of 23.72 σ_T. Density was also much less variable in 2012

than in 2013: the range of all density values measured over the four days of sampling was much smaller in 2012 (0.28 σ_T) than in 2013 (0.58 σ_T). Finally, neither ebb-flood nor spring-neap scales of tidal variation showed significant correlation with water density in 2012 (Figures 6b and 7a).

DISCUSSION

The spatial dimension of these data represented by depth gives insight into how water mixing takes place in the southern part of the San Juan Channel. The intrusion of oceanic water into an estuarine system can occur in a variety of ways. In highly stratified systems, exchange is minimal between a low-density surface layer (freshwater input) and the high-density bottom layer (oceanic input). (Mann and Lazier 1991) However, in the tidally-mixed environment of the San Juan Channel, tidal currents are strong enough to mix the entire water column so that no pycnocline is present. The gradual and significant change in density over time observed in this study indicates that denser oceanic water was being mixed into the less dense channel water, rather than simply sinking below it. This is supported by the measurements of physical water properties down to 20m that indicate a mostly homogeneous water column. The mixed water column can be further understood as the result of turbulent mixing caused by the interaction of currents and bathymetry. Such mixing has been shown to occur on the downcurrent side of a shallow sill (Itoh et al 2011), and can similarly be expected at the Griffin Bay site, due to its location just north of a shallow sill at Cattle Pass.

A few casts measured a water column in which density varied distinctly by depth. However, they did not exhibit the stable, stratified structure that typically characterizes

such heterogeneity. Rather, water at depth was less dense than shallower water. Since denser water sinks, this arrangement is unstable, and thus evidence of mixing in process.

The result that water density increases with time since slack low is consistent with previous understanding of tides' effect on physical water properties at this location. Within a single flood tide, the amount of oceanic water that has entered the channel is more closely dependent on how long the flood tide has been in progress than on the speed of the current. The similar range in density from slack low to fast flood over the four days of sampling, despite differences in maximum current speed, shows that the primary contributor to the increase in density is not current speed; rather, time and current direction control how much cold water has been pushed into the channel.

The decrease in water density observed around the time of the fast flood on the final three days of sampling is indicative of a pulse of warmer, fresher water. However, it is distinct from the freshwater pulse at the leading edge of the tidal front seen on some days in 2012, which was hypothesized to be a signal from the Columbia River (Eisenlord 2012). The 2013 freshwater signal occurred later in the flood tide, was weaker and of shorter duration. The fact that the 2013 pulse, although less dense than the water immediately before it, still fell within the range of other values at that location for the day indicates that it was not a separate, external signal but a less dense part of the two water masses already present in the channel. The timing of the 2013 freshwater pulse coincides with the appearance of the heterogeneous and unstable water masses discussed above. Thus, one possible interpretation of the 2013 freshwater pulse is as the mixing in of additional channel water that had not previously made it to the sampling location, but was advected there after peak flood due to turbulence caused by increased current speed.

Physical water properties are affected not only by the progress of the current tidal phase but by the condition of the water at the start of that phase, which depends on the relative strength of previous ebbs and floods. This varies on a spring-neap cycle and was quantified in this study by the measurement of previous tidal range, which indicates how much channel water was replaced by oceanic input during the previous day. Greater values of previous tidal range signify a greater oceanic input, and thus would be expected to correlate with greater density.

The 2013 data support this hypothesis. As tidal condition transitioned from neap to spring over the four days of sampling, exchanges – and thus values for previous tidal range – increased. Due to the greater exchange, the water already in the channel at the beginning of the flood tide was denser later in the week. This was reflected in the measurements of conditions at the start of flood tides each day, which found an increase in average density at slack low over the four days of sampling. The different starting conditions affected not only the first measurement each day but all subsequent measurements, as shown by the linear regression which attributed 33% of overall variation in density over the four days to previous tidal range.

In 2013, the ebb-flood and spring-neap scales of tidal variation were about equally important in determining density. Together they explained 62% of the variation in density over the sampling period. Causes of the remaining variability are outside the scope of this study but may have included changing weather conditions and micro-scale water dynamics.

In order to correctly interpret differences in physical water properties at Griffin Bay between 2012 and 2013, it is necessary to understand the global climate processes

that form the context for these observations. The El Nino Southern Oscillation (ENSO) creates annual differences in climate due to varying ocean circulation and atmospheric conditions. The 2012 ENSO status was neutral but followed two years of La Niña, which cause cooler temperatures in this region. The 2013 ENSO status was also neutral. (http://www.cpc.ncep.noaa.gov/products/analysis_monitoring/ensostuff/ensoyears.shtml). The Pacific Decadal Oscillation (PDO) fluctuates between cool and warm effects on a decade-long cycle, and in 2012 the PDO had been cool for three successive years. (http://jisao.washington.edu/pdo/PDO.latest) Perhaps due to these compounding effects, sea temperatures were unusually cool in the southern San Juan Channel in the fall of 2012 (Figure 8), contributing to the high density of water at Griffin Bay in the 2012 study. Salinity values were also somewhat greater in 2012 than 2013, although the reason for this difference is unknown. However, despite the fact that salinity rather than temperature typically drives density variation in estuarine regions, salinity variation in this case had a lesser impact on density because the difference in salinity between 2012 and 2013 was much less significant than the difference in temperature.

Because water in the channel in 2012 was colder and saltier, it more closely resembled the incoming oceanic water than in 2013. This can be seen in the ranges of typical October values for stations N and S in 2012 and 2013 (Figure 4). Station N, influenced by input from the Georgia Strait and Fraser River, is representative of the nearshore water mass, while station S indicates the condition of the oceanic input. In 2013, the regions of the temperature-salinity plot typically occupied by water at the two stations are completely disjoint, indicating a large difference in the two water masses undergoing tidal mixing at Griffin Bay. This difference can be seen in the range of

density values measured during small-scale sampling: measurements taken near slack low resemble oceanic water, while those taken later in the flood tide more closely resemble channel water. Since the two water masses have very distinct properties, a large range of intermediate values is seen. By contrast, in 2012 the characteristics of physical oceanography at stations N and S overlap, indicating that the two water masses mixing at Griffin Bay were similar to each other. This is confirmed by the smaller range of density values found at Griffin Bay in 2012.

The lack of significant relationship between tidal conditions and water density in 2012 is best interpreted not as a lack of mixing, but as the mixing of two similar signals. It is expected given this context, and does not contradict the relationship seen in 2013. Because the two water masses meeting in the southern San Juan Channel in 2012 had similar physical properties, the gradient between them caused by mixing was small. Thus, changes in density that did occur due to tidal mixing were likely masked by uninvestigated sources of variability (such as weather and micro-scale water circulation) that were also seen to be important in 2013.

Although conditions in 2013 were such that the observations in this study clearly illustrated the expected pattern, the difference in response of physical water properties to tidal variation in 2012 and 2013 indicates the need for further work to understand and quantify the effects of external factors such as climate. A more complete understanding of how physical water properties are affected by ebb-flood, spring-neap and interannual climatic changes will further serve as important context for tidally-influenced dynamics of the chemical and biological aspects of the ecosystem.

REFERENCES

Bernard, G.A. 2010. Effects of tides and remote forcing on oceanographic properties within the San Juan Channel during early fall. University of Washington Friday Harbor Laboratories Pelagic Ecosystem Function Research Apprenticeship.

Eisenlord, M.E. 2012. Fine temporal scale sampling of tides, water masses, and seabirds. University of Washington Friday Harbor Laboratories Pelagic Ecosystem Function Research Apprenticeship.

Harmann, A. 2008. The effects of tides on water column structure, dissolved oxygen, and zooplankton abundance at Cattle Pass, Washington. University of Washington Friday Harbor Laboratories Pelagic Ecosystem Function Research Apprenticeship.

Itoh, S., I. Yasuda, M. Yagi, S. Osafune, H. Kaneko, J. Nishioka, T. Nakatsuka, Y. Volkov. 2011. Strong vertical mixing in the Urup Strait. Geophysical Research Letters 38.

Mann, K.H., J.R. Lazier. 1991. Dynamics of Marine Ecosystems: Biological-Physical Interactions in the Oceans. Blackwell Scientific Publications: Boston, Massachusetts, USA.

Thomas, K. 2011. Seasonal and tidal effects on water density gradients in the San Juan Channel. University of Washington Friday Harbor Laboratories Pelagic Ecosystem Function Research Apprenticeship.

Thompson, J. 2013. Annual and interannual patterns of physical oceanographic properties in the San Juan Channel. University of Washington Friday Harbor Laboratories Pelagic Ecosystem Function Research Apprenticeship.

Tolkin, T. 2007. Seasonal variability in temperature, salinity, dissolved oxygen and nutrients content in the San Juan Channel in Fall, 2007. University of Washington Friday Harbor Laboratories Pelagic Ecosystem Function Research Apprenticeship.

Williams, K. 2012. Spatial and temporal variation in hydrography, chlorophyll, and oxygen of San Juan Channel: effects of local and external factors. University of Washington Friday Harbor Laboratories Pelagic Ecosystem Function Research Apprenticeship.

TABLES AND FIGURES

Table 1. Tidal conditions during October R/V Centennial cruises

2012		2013	
Date	**Tide**	**Date**	**Tide**
10 Oct	Flood	9 Oct	Ebb
17 Oct	Ebb	15 Oct	Slack
20 Oct	Flood	22 Oct	Ebb
30 Oct	Ebb	29 Oct	Flood

Figure 1. Map of study area, showing Griffin Bay small-scale oceanography sampling site and R/V Centennial stations N and S.

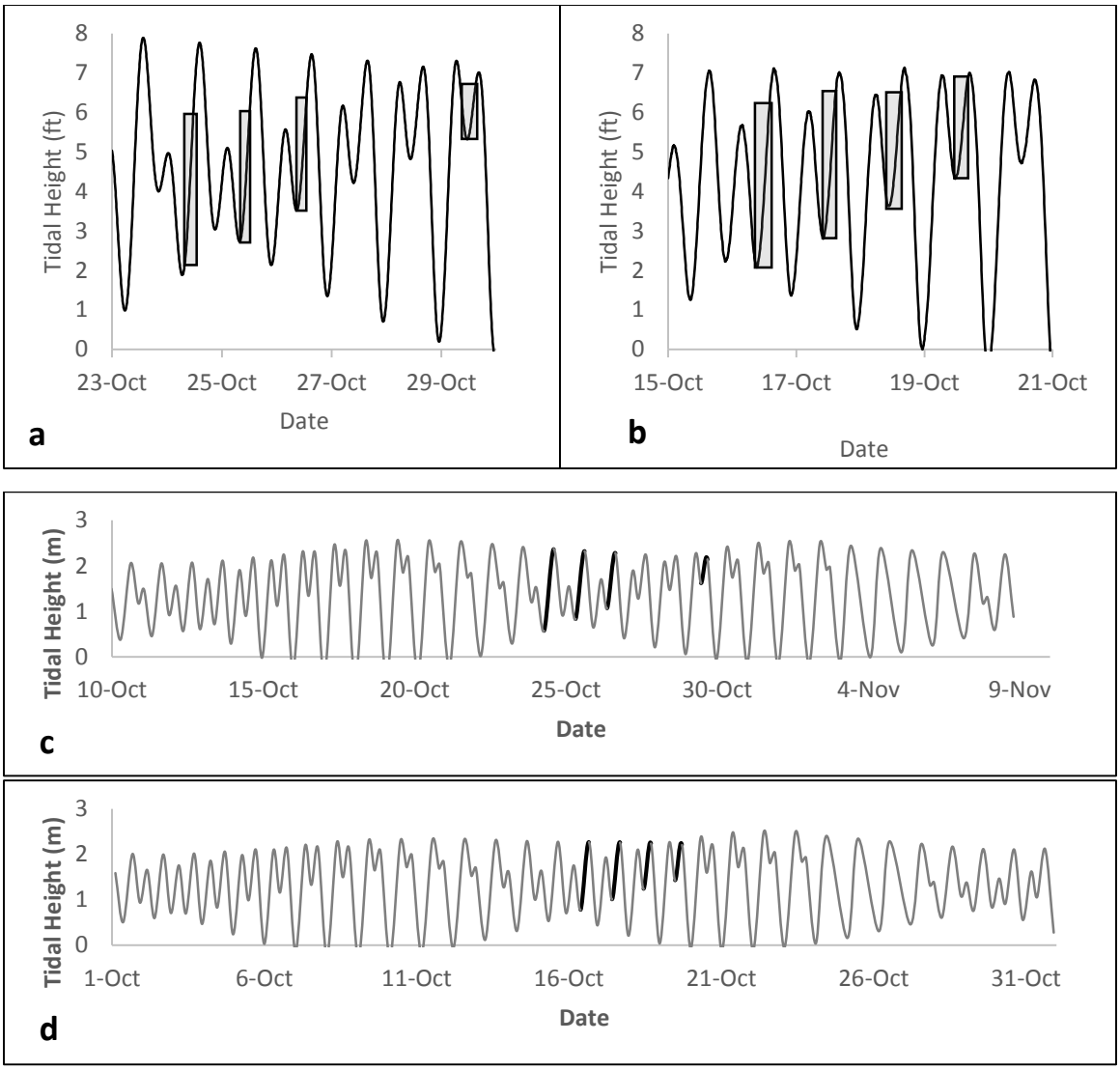

Figure 2. Tidal conditions during sampling, at ebb-flood scale in (a) 2012 and (b) 2013, with sampling times denoted by gray boxes. At spring-neap scale in (c) 2012 and (d) 2013, with sampling tides denoted in red.

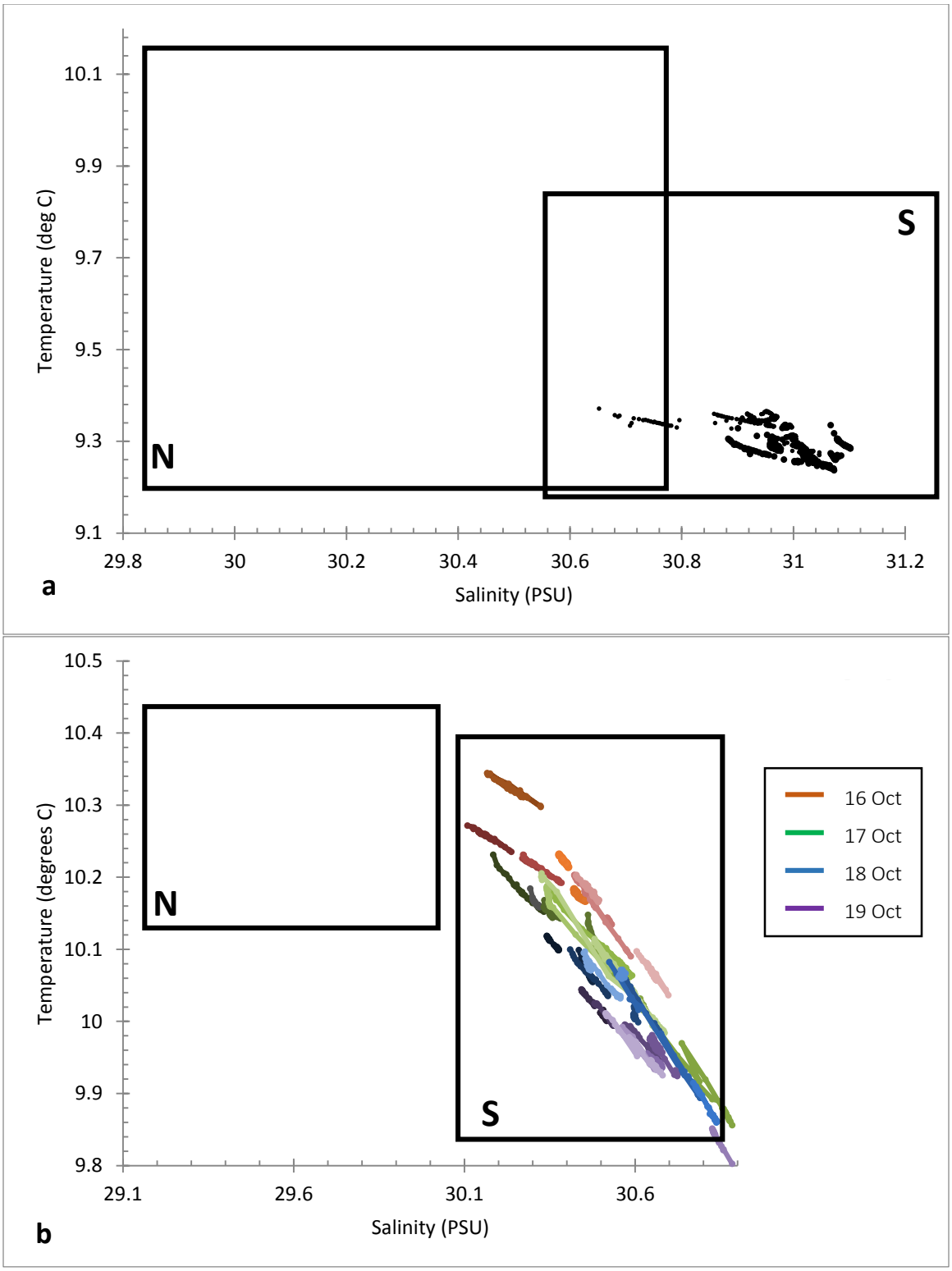

Figure 3. Temperature and salinity from small-scale sampling at Griffin Bay site. Boxes bound values within one standard deviation of means at stations N and S, based on October Centennial data down to 20m depth, in (a) 2012 and (b) 2013.

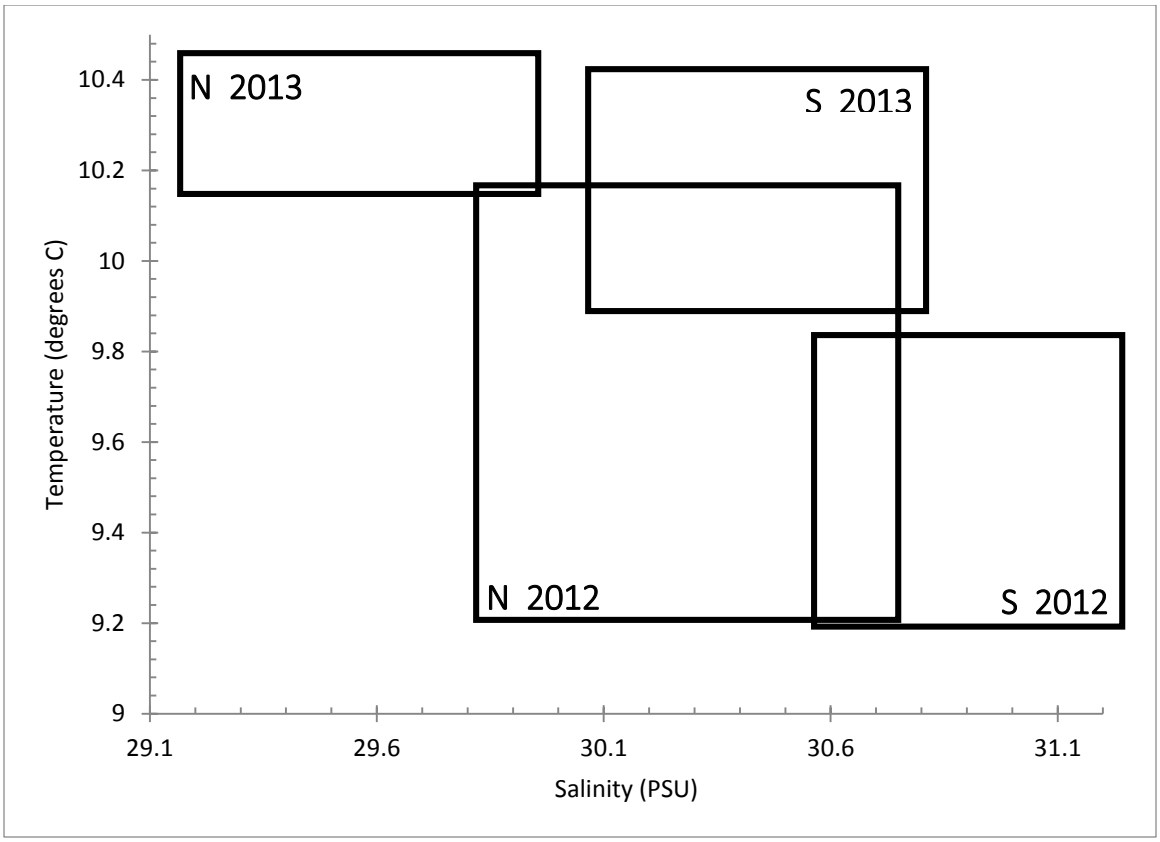

Figure 4. Boxes bound values within one standard deviation of mean temperature and salinity values in the top 20m of the water column at stations N and S, as measured in October 2012 and 2013 by the R/V Centennial.

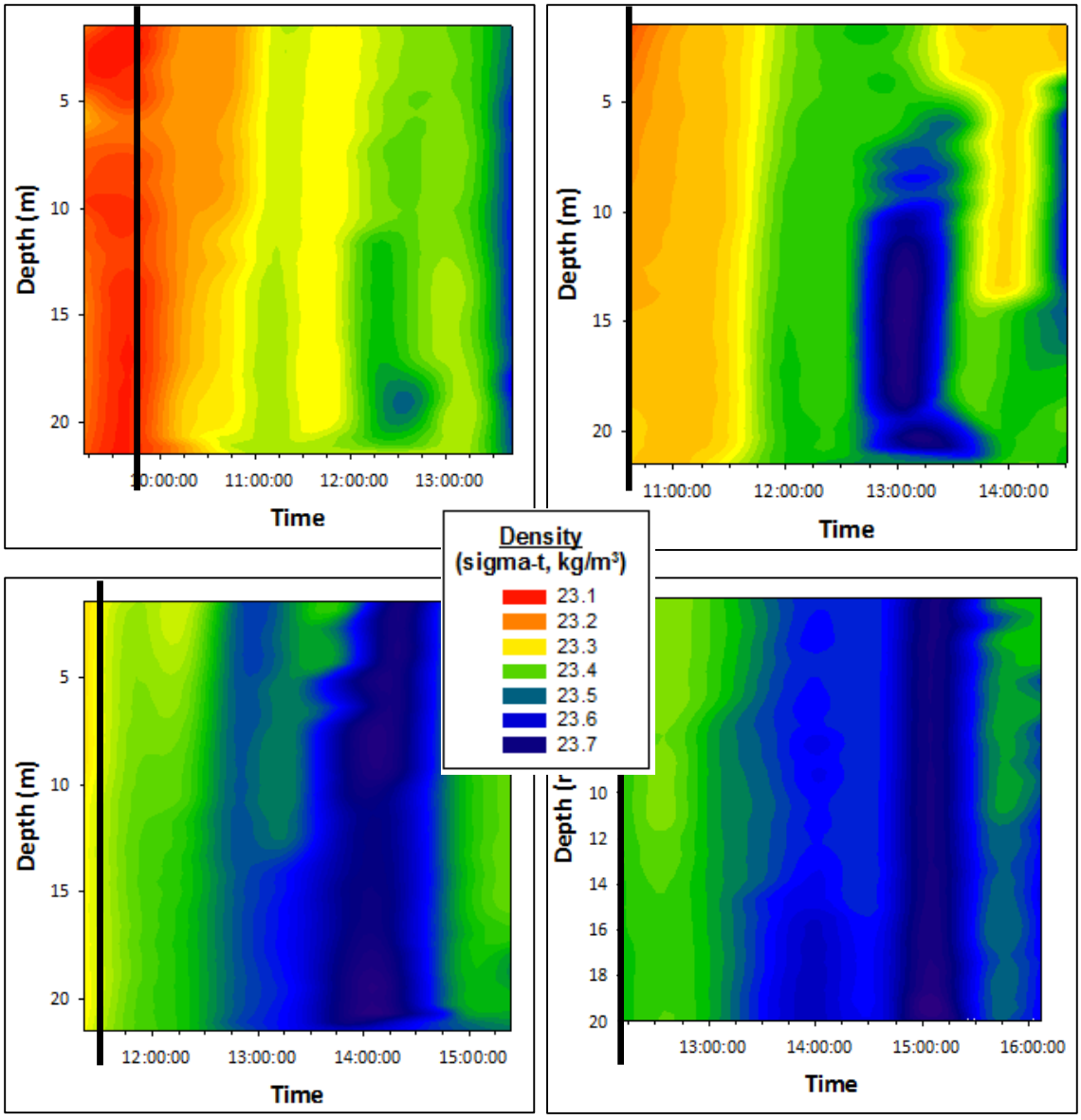

Figure 5. Contour plots of seawater density, with time of slack low tide indicated by vertical line, for sampling dates in 2013: (a) 16 October, (b) 17 October, (c) 18 October, (d) 19 October.

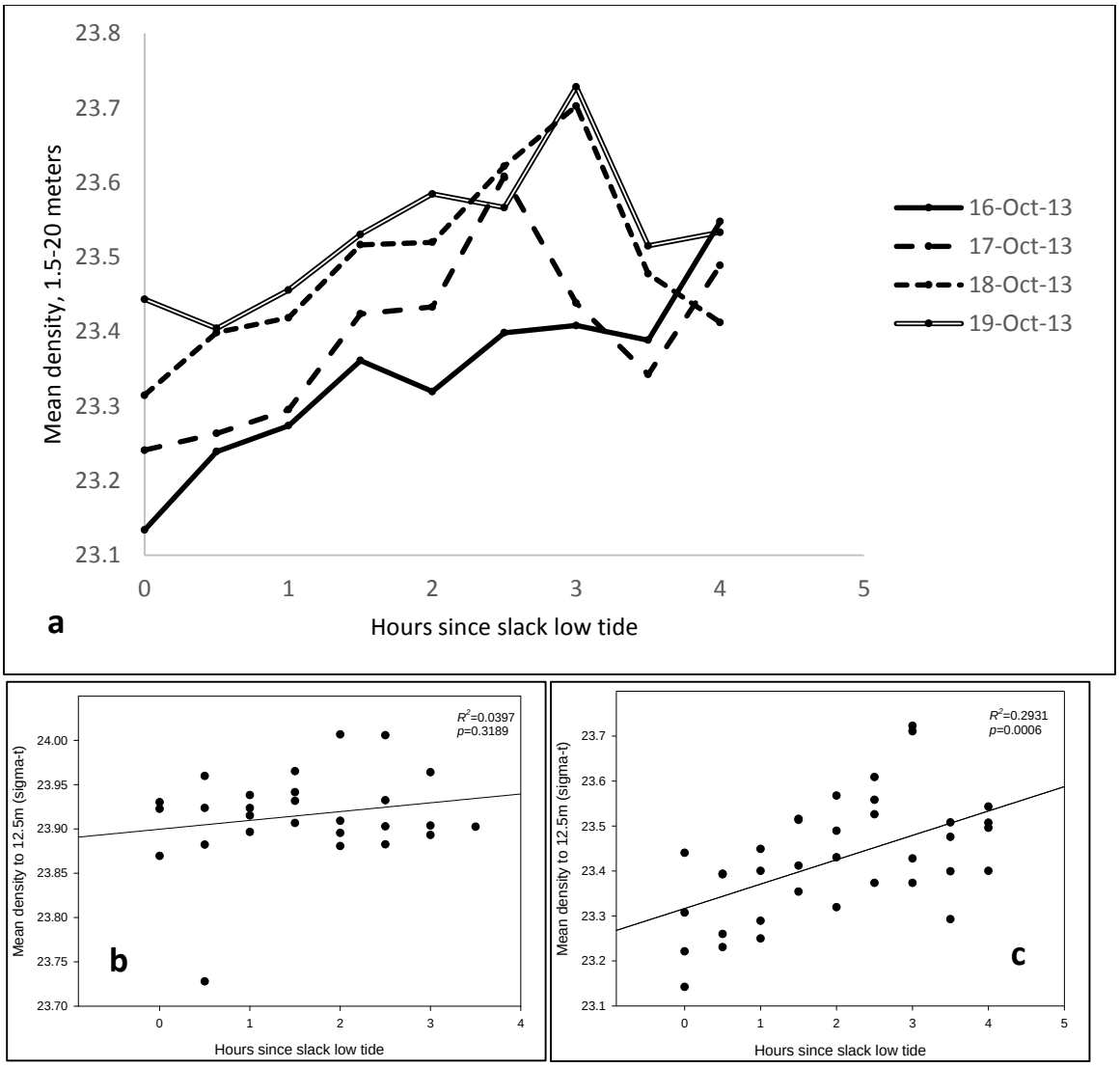

Figure 6. Slack-flood tidal effects on density: (a) separated by day in 2013; and for all days combined in (b) 2012 and (c) 2013.

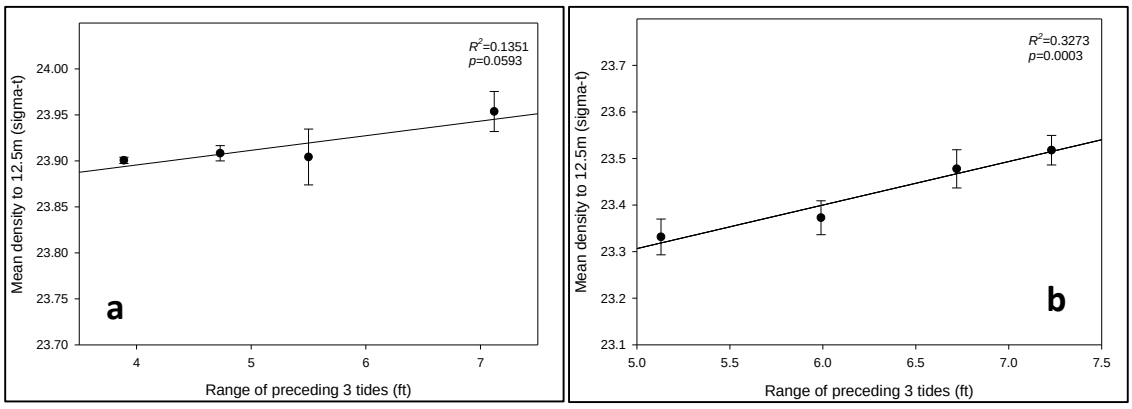

Figure 7. Spring-neap tidal effects on density in (a) 2012 and (b) 2013.

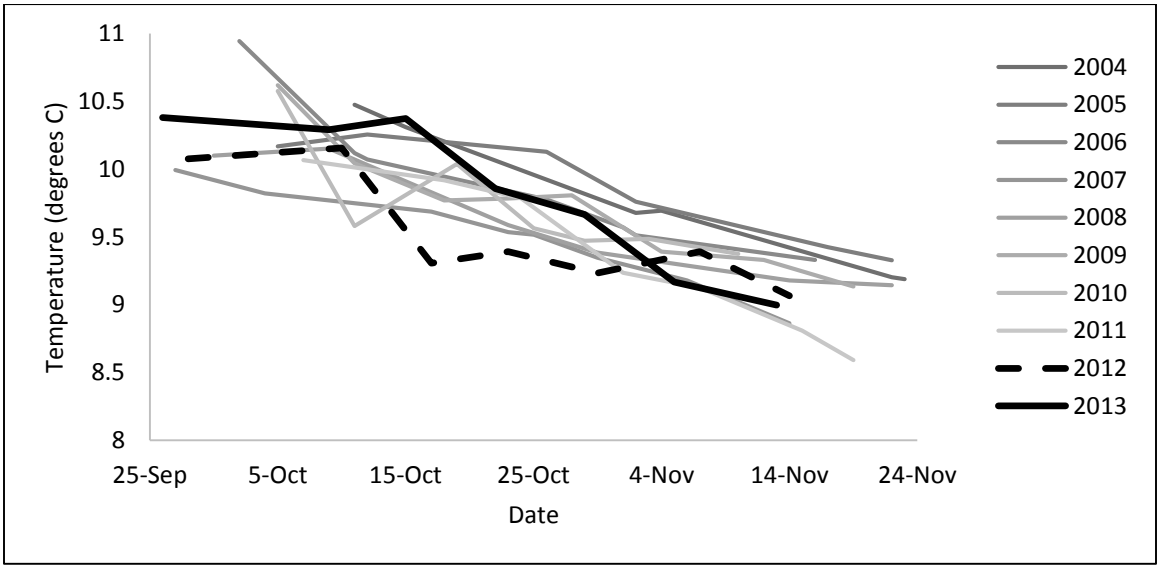

Figure 8. Average sea temperatures at 20m depth at R/V Centennial station S.

Part II: Tidally-mediated effects of bathymetry on seabird distribution in the San Juan Channel

ABSTRACT

Interactions of ocean currents and bathymetry have been shown to create concentrations of prey, which in turn attract predators. The varied and well-documented bathymetry and abundant seabird populations of the San Juan Channel provide a particularly rich opportunity to examine these interactions in a nearshore, tidally active area. In the present study, my objective was to investigate the relationship between bathymetry, tides and seabird distribution. To do this, I used two sets of methods: description of seabird distribution at a detailed scale using survey transect data, and characterization of the bathymetry of the channel by statistical measures at the same scale. Initial analysis of these data revealed evidence of seabird aggregation influenced by tidal interaction with bathymetry. These results suggest that further analysis and improvements in the methods developed have the potential to reveal additional interesting patterns.

INTRODUCTION

Through its effects on local ocean circulation, bathymetry influences the distribution of nutrients, predators, and prey in pelagic ecosystems. When water at depth encountering an abrupt bathymetric feature is forced upward, nutrients and plankton previously confined to deeper layers are vertically distributed by the resulting turbulence, attracting predators (Hunt et al 1999). This effect has been observed at features such as seamounts (Lueck 1997), undersea canyons and continental shelf-breaks (Yen et al 2004).

A special case occurs in nearshore areas where tidal currents interact with shallow sills, such as at Cattle Pass in the south end of the San Juan Channel. Tides move water across the sill, northward into the channel during flood tides and outward to the south during ebbs. The water movement creates particularly high turbulence on the downcurrent side of the sill, with an associated increase in prey and predators (Zamon 2000). This effect, known as the tidal coupling hypothesis, is an example of how tidal

conditions and bathymetry combine to create suitable habitat for predators. Better knowledge of it is important for understanding the local ecology, and has implications for monitoring and management of the ecosystem.

How significant are the effects of bathymetry in a nearshore, bathymetrically heterogeneous system? In addition to the Cattle Pass sill, the San Juan Channel exhibits a wide variety of bathymetric features. Past research has shown great spatial variability within the channel in characteristics from physical oceanography to seabird abundance (Williams 2012, Palmquist 2011), but not at fine enough scale to allow for comparison to bathymetry. The present study was conducted to investigate the extent to which ecological variation in the San Juan Channel can be explained by tidal interaction with bathymetry. In particular, I consider seabird distribution as an indicator of ecosystem response.

The broad goal of this study was to investigate the viability and methods of studying the relationship between seabird distribution and bathymetry. Specific objectives were as follows:

- Collect seabird abundance data for the ongoing PEF dataset and use 2012 and 2013 data to extract distribution information at a small spatial scale
- Develop measures to characterize the bathymetry of the San Juan Channel
- Investigate the relationship between seabird distribution and bathymetry

METHODS

Bird Abundance Surveys

Bird abundance was measured using a strip transect method aboard the R/V Centennial on weekly cruises during the autumns of 2006-2013. Surveys were conducted

while traveling at an average speed of 8 knots along a 22-km transect (see Figure 1). Both northbound and southbound traversals of the route occurred and were included in the data.

Observers stationed at 3 meters above the water level on the port and starboard sides of the bow counted birds and marine mammals within 200m on either side of the vessel (as estimated by the observers). All sightings were identified to lowest taxa possible. The time of each observation was recorded to the nearest minute. In 2012 and 2013 flight direction was recorded, when applicable, for birds in all families except Laridae.

Bins

The R/V Centennial survey route was approximated by a piecewise linear path with four vertices (see Table 1). The area surveyed, based on this approximation, was divided into 21 rectangular bins, numbered from north to south (Figure 1). Bins were defined with a length of 1km parallel to the transect and a width of 0.4km perpendicular to the transect. A final bin at the south end of the transect (bin #22) covered the remaining 0.3983km of transect length.

Each bird observation was assigned to a bin using the following formula:

For southbound transects:

$$Bin = \left\lceil L * \frac{t_{obs} - t_{start}}{t_{end} - t_{start}} \right\rceil$$

For northbound transects:

$$Bin = \left\lceil L * (1 - \frac{t_{obs} - t_{start}}{t_{end} - t_{start}}) \right\rceil$$

where $L = 21.3983$ km is the length of the transect, t_{obs} is the time of the observation and t_{start} and t_{end} are the beginning and ending times of the transect, respectively.

Measures of Bathymetry

Thirteen measures (summarized in Table 2) were used to describe the bathymetry of the area covered by the bins. All measures except rugosity and minimum channel width were calculated for each bin by John Aschoff based on bathymetry data from H. Gary Greene. Rugosity and minimum channel width were estimated visually from maps generated by H. Gary Greene and John Aschoff. No minimum channel widths were estimated for bins 19-22 because these bins fall outside the southern end of the channel.

Data Analysis

Bin assignments were made for all complete and continuous transects in the PEF database from 2006 to 2013, but only data from the 13 transects in 2012 and 2013 were used for analysis. Birds in flight (except gulls) were excluded from analysis. The number of birds observed in bin 22 was multiplied by a factor of 2.5 to account for the smaller size of bin 22 and allow for comparison with other bins. The total number of birds sighted during the 13 transects was calculated for each bin (with subtotals by family), and these totals were compared by linear regression against each bathymetric measure.

Bin totals were subdivided in two ways for further analysis. Because port and starboard observations were recorded separately, it was possible to divide observation data according to whether a bird was seen in the east or west side of a bin. Each transect was also classified according to tidal phase. Transects that took place entirely during a

single phase (either flood or ebb), according to NOAA tidal current predictions for Turn Rock (http://tides.mobilegeographics.com/locations/6623.html), were classified as flood or ebb accordingly. Transects that spanned both flood and ebb were classified as slack.

RESULTS

The analysis of bird distribution data by bin revealed great spatial variability throughout the channel (Figure 2). In the 13 transects from 2012 and 2013, the bin with the least number of birds (bin 1) had 108, while the bin with the most (bin 21) had 2495. Only two bins (20 and 21) had more than 800 birds. Different families appeared to show different patterns of spatial variation, but a single family was chosen for further analysis. Although gulls and alcids were about equally numerous (6787 gulls and 6545 alcids), alcids were selected because they showed greater variation and alcids flying overhead could be excluded from analysis. Bin 1 had the fewest alcids (26), while bin 21 had the most (1562). Only three bins (20, 21 and 22) had alcid abundance greater than 400.

Linear regressions comparing bird abundance to bathymetric measures in each bin were almost all insignificant. Several representative examples are shown in Figure 3a, c and d. The only exception was minimum channel width estimate (Figure 3b). A positive correlation between minimum channel width and alcid abundance was found, with $p=0.0256$ and $R^2=0.2746$. All other p-values were greater than 0.05.

Most bins were roughly symmetrical in the number of alcids seen on the east and west sides, but a few exceptions were noted. Considerably more birds were seen on the west side in bins 4, 7, 20 and 21 (Figure 4). The west sides of bins 4, 20 and 21 are distinguished by steep dropoffs not present on the east sides (Figure 1).

Separation of bin totals by tidal phase indicated new patterns (Figure 5). Abundance results showed more total birds during flood tides than ebbs. A total of 4961 birds were observed on the 6 transects conducted on ebb tides, while 9098 birds were counted during the 6 flood tide transects. There were also clear differences in distribution according to tide. During flood tides, alcid totals spiked in bins 3-4, 10-11, 15-16 and 21. Ebb tide spikes occurred just to the south of these locations, in bins 6, 12-13 and 20-22.

A combination of two measures of bathymetry identified areas of the channel that appear to be linked to the ebb-flood differences in alcid distribution. Based on the calculated bathymetric measures, the only bins with both high rugosity (as measured by standard deviation of depth) and narrow channel width were 5-6 and 17-18 (Figure 6). These bins describe the locations of a sill in the northern part of the channel and the Cattle Pass sill in the south (Figure 1). Distribution results showed alcids to be more numerous to the north of these locations on flood tides, and to the south of them on ebb tides.

DISCUSSION

The lack of statistically significant correlations between bathymetric measures and bird distribution may not be proof of a lack of relationship between seabirds and bathymetry, but rather an indication that more work needs to be done to understand that relationship. Several preliminary findings support this idea and suggest methods for improvement.

A high maximum slope indicates a steep dropoff, which has been associated with mixing and turbulence (Wolanski and Hamner 1988); thus, high values for maximum

slope were hypothesized to correlate with high bird abundance. Although a comparison of maximum slope to bird abundance in each bin did not show this as a consistent pattern throughout the channel (Figure 3a), the east-west pattern of bird distribution in bins 4, 20 and 21 indicated a possible response to steep dropoffs. One possible reason for this discrepancy is that maximum slope is too sensitive a measure: it detects features that are steep but too small to be of any consequence to predators at the surface. Some other measure indicating the presence and extent of steep dropoffs in a bin might be more effective.

Rugosity was hypothesized to interact with tidal currents to increase turbulence, creating greater mixing and making food available to predators at the surface. Standard deviation of depth provided an estimate of depth variation within each bin, and so was used as a proxy for rugosity. It performed similarly to a subjective estimate of rugosity based on visual examination of a hillshade map (Figures 3c and 3d), and was thus judged as roughly reliable. However, many other measures of surface roughness are possible (Grohmann et al 2011), and further investigation will be required to determine which is best suited to the conditions of this study.

The width of a channel is known to affect the velocity of water flowing through it: narrow channels cause fast currents which in turn create greater turbulence and mixing, hypothesized to lead to increased predator abundance. The positive correlation between minimum channel width and alcid abundance (Figure 3b) would seem to suggest the opposite; however, this result must be interpreted in the context of tides, as discussed below. Channel width in this study was estimated visually using a map and ruler; a more accurate and precise method would be desirable. The minimum channel width for each

bin was used because presence of a narrows and the accompanying fast current was thought to have a more direct effect on bird abundance than presence of a very wide area. However, maximum, mean or other measures of channel width (perhaps taking into account the suddenness of widening or narrowing) may be useful.

Division of the data by tides confirmed relationships of tidal phase to both abundance and distribution of seabirds in the San Juan Channel. Data from 2012 and 2013 agree with previous studies showing greater overall bird abundance in the channel on flood tides (Zamon 2000, Spatz 2007). This can be attributed to the influx of prey-rich oceanic waters from the Strait of Juan de Fuca, and also possibly from Strait of Georgia (Kull 2008). High rugosity and narrow channel width were both hypothesized to correlate with high predator abundance, and the use of these two measures together clearly identified two regions of the channel that had a tidally-mediated effect on bird distribution. The high bird abundance found to the north of these regions on flood tides, and to the south on ebb tides, supports the theory that greater predator abundance occurs downcurrent of a sill. Thus, these data offer further support for the application of Zamon's tidal coupling hypothesis to Cattle Pass, and the first evidence for its effects at the north end of the channel.

The resolution at which seabird data are processed should be considered, because the choice of bin size may cause some patterns to be emphasized and others hidden. Patterns in distribution of seabirds have been described at multiple scales, ranging from hundreds of kilometers to 1 kilometer, based on different processes causing prey also to be distributed at multiple scales (Fauchald et al 2000). If distribution is not analyzed at a scale that matches the process of interest, patterns may be obscured. Burger et al (2004)

found that diving and surface-feeding birds off the southwest coast of Vancouver Island aggregate in response to prey at scales of 2 to 8 km, and therefore recommended that surveys use a resolution of 1 to 10km. While the present study falls within that range, it is possible that the dominant processes in the environment of the channel work on different scales than those of the continental shelf. Thus, further work on this subject should include analyses to determine spatial scales of aggregation of seabirds in the San Juan Channel. This might include a modification of survey methods: greater precision in data collection would be necessary for analysis with bin sizes much smaller than 1km to be meaningful.

This study demonstrated measures that can be effective in describing the bathymetry of the San Juan Channel, and that a relationship exists between the properties captured by these measures and seabird distribution. Analysis of bird distribution data on the scale of 1-km bins revealed patterns that had not been evident in previous PEF work. Furthermore, it demonstrated that the relationship between seabirds and bathymetry cannot be clearly understood without considering tides.

However, the analyses performed here are only a first attempt and many improvements are possible. As discussed above, an investigation of the effect of varying bin size might be useful. Also, while simple regressions based on bathymetric measures were not effective in predicting bird distribution, the success of combining two of these measures with tidal data suggests directions for further work. A generalized linear model incorporating many bathymetric features and considering tidal conditions could provide a more powerful tool for understanding the relative importance of different bathymetric

characteristics. Such a model might incorporate new bathymetric factors not yet addressed, or, as discussed above, refinements of the ones used here.

This work leaves open many related questions about other components of the San Juan Channel ecosystem. The response of seabird distribution to bathymetry is indirect, mediated not only by tidal conditions but by many other levels of the ecosystem including physical and chemical oceanography, plankton and forage fish. Much work is yet to be done to understand how each of these components is affected by bathymetry and the role each plays in tidal coupling.

REFERENCES

Burger, A.E., C.L. Hitchcock, G.K. Davoren. 2004. Spatial aggregations of seabirds and their prey on the continental shelf off SW Vancouver Island. Marine Ecology Progress Series 283: 279-292.

Fauchald, P., K.E. Erikstad, H. Skarsfjord. 2000. Scale-dependent predator-prey interactions: the hierarchical spatial distribution of seabirds and prey. Ecology 81:773-783.

Grohmann, C.H., M.J. Smith, C. Riccomini. 2011. Multiscale analysis of topographic surface roughness in the Midland Valley, Scotland. IEEE Transactions on Geoscience and Remote Sensing 49: 1200-1213.

Hunt, G.L., F. Mehlum, R.W. Russell, D. Irons, M.B. Decker, P.H. Becker. 1999. Physical processes, prey abundance, and the foraging ecology of seabirds. 2040-2056 *in* Adams, N.J. and R.H. Slotow, editors. Proc. 22 Int. Ornithol. Congr., Durban. BirdLife South Africa, Johannesburg.

Kull, K. 2008. Fall influence of the Fraser River in the San Juan Archipelago. University of Washington Friday Harbor Laboratories Pelagic Ecosystem Function Research Apprenticeship.

Lueck, R.G. 1997. Topographically Induced Mixing Around a Shallow Seamount. Science 276: 1831-1833.

Palmquist, D. 2011. Distribution and abundance of Marbled Murrelets in the San Juan Channel. University of Washington Friday Harbor Laboratories Pelagic Ecosystem Function Research Apprenticeship.

Spatz, D.R. 2007. Tidal effects on the distribution and abundance of seabirds in the San Juan Archipelago, Washington. University of Washington Friday Harbor Laboratories Pelagic Ecosystem Function Research Apprenticeship.

Williams, K. 2012. Spatial and temporal variation in hydrography, chlorophyll, and oxygen of San Juan Channel: effects of local and external factors. University of Washington Friday Harbor Laboratories Pelagic Ecosystem Function Research Apprenticeship.

Wolanski, E., W.M. Hamner. 1988. Topographically controlled fronts in the ocean and their biological influence. Science 241: 177-181.

Yen, P.P., W.J. Sydeman, K.D. Hyrenbach. 2004. Marine bird and cetacean associations with bathymetric habitats and shallow-water topographies: implications for trophic transfer and conservation. Journal of Marine Systems 50: 79-99.

Zamon, J.E. 2000. The influence of tidal currents on plankton densities and energy flow to seals, seabirds, and schooling fishes in the San Juan Islands, WA. University of California, Irvine, Doctoral Dissertation.

TABLES AND FIGURES

Table 1. Locations of vertices of piecewise linear path approximating Centennial transect. Vertices are listed north to south (see Figure 1).

Vertex Name	Latitude	Longitude
N	48.583	-123.042
B	48.523	-122.945
C	48.483	-122.958
S	48.42	-122.943

Table 2. Measures used to describe bathymetry of bins.

Descriptive Measure	Source	Minimum Value	Maximum Value
Mean Aspect	Calculated by John Aschoff based on bathymetry and substrate data from Gary Greene	78.13	224.86
Standard Deviation of Aspect		47.49	125.35
Maximum Slope		3.17	81.85
Mean Slope		1.12	20.19
Standard Deviation of Slope		0.53	13.87
Minimum Depth		-170.55	-82.36
Maximum Depth		-126.60	-6.65
Range of Depth		8.74	115.46
Mean Depth		-146.02	-49.69
Standard Deviation of Depth		1.79	33.58
Percent Soft Substrate		0.04	1.00
Minimum Channel Width	Estimate	2	11
Rugosity	Estimate	1	8

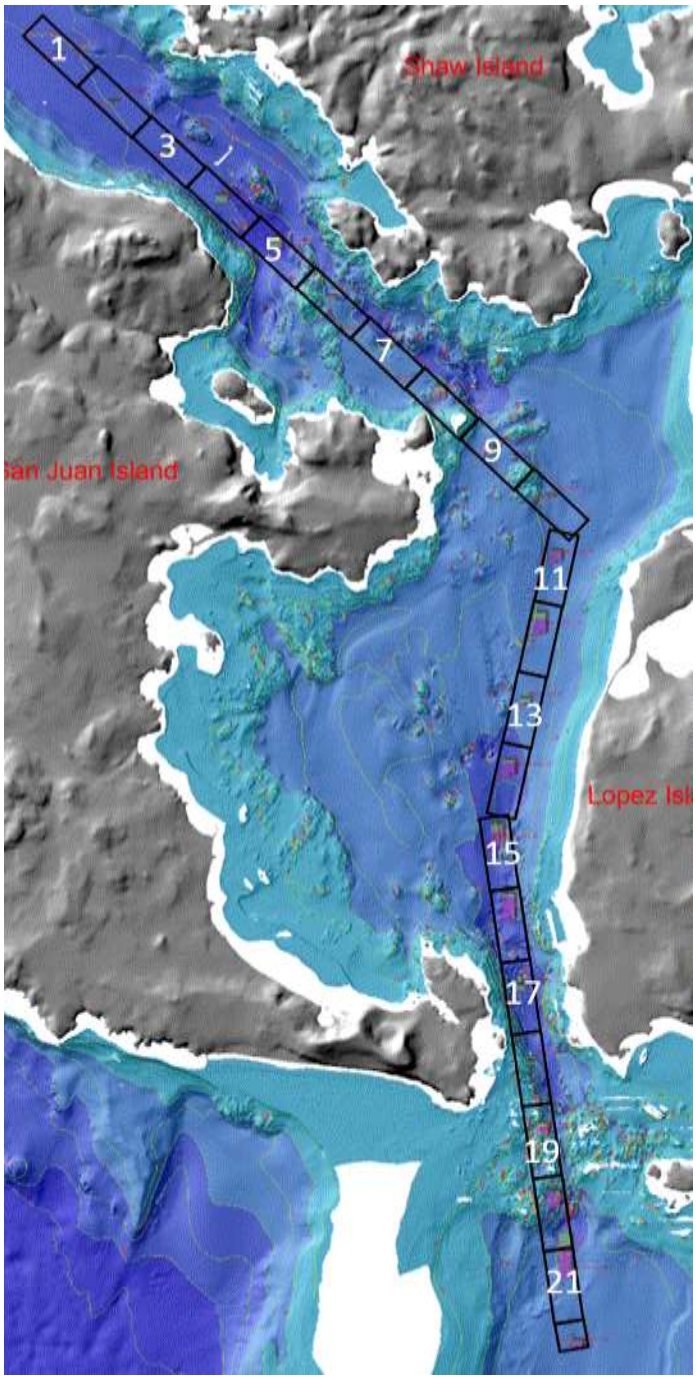

Figure 1. Bathymetry of study area, and division of transect into numbered bins.

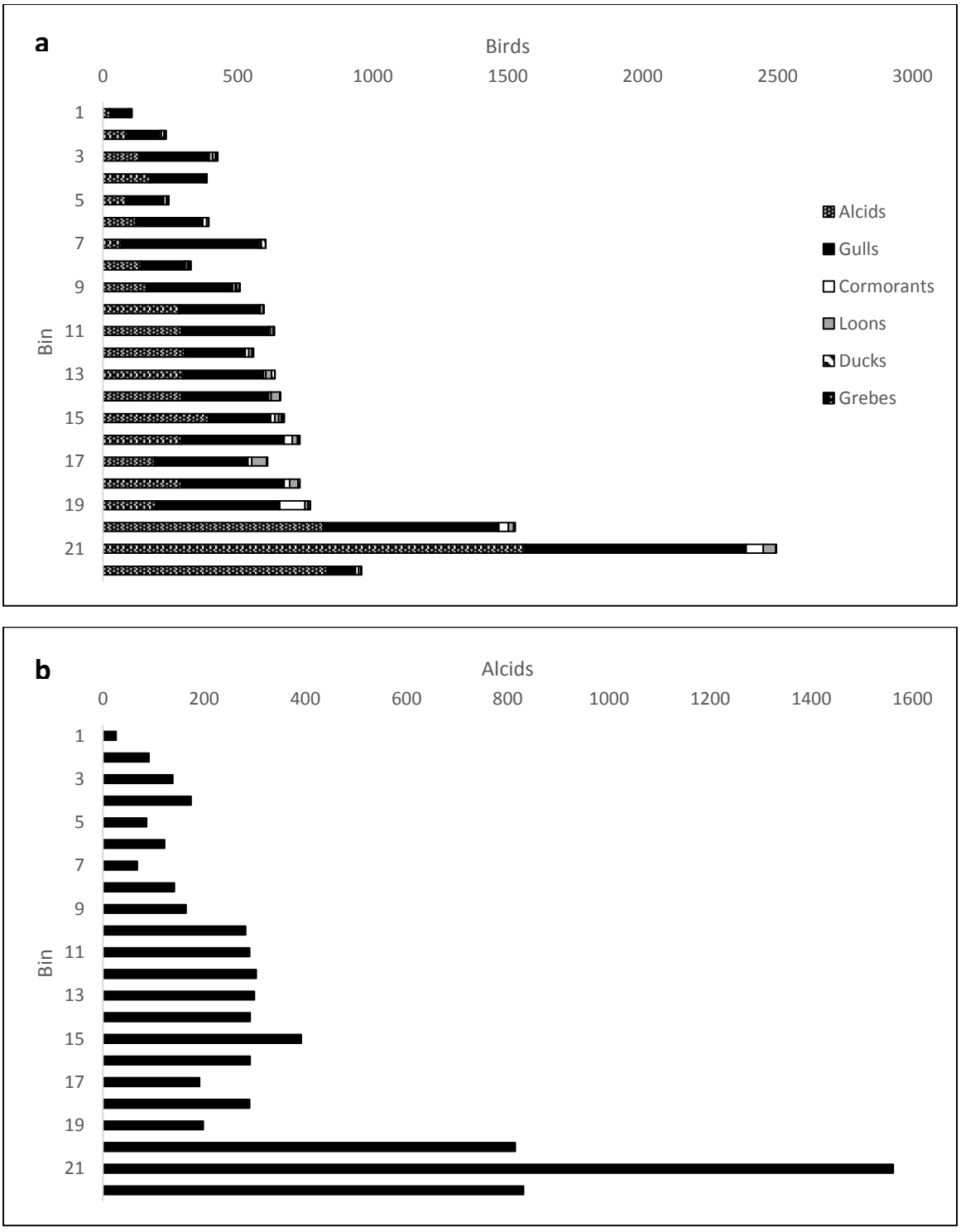

Figure 2. Total number of (a) birds and (b) alcids recorded in each bin during complete and continuous transects in 2012 and 2013.

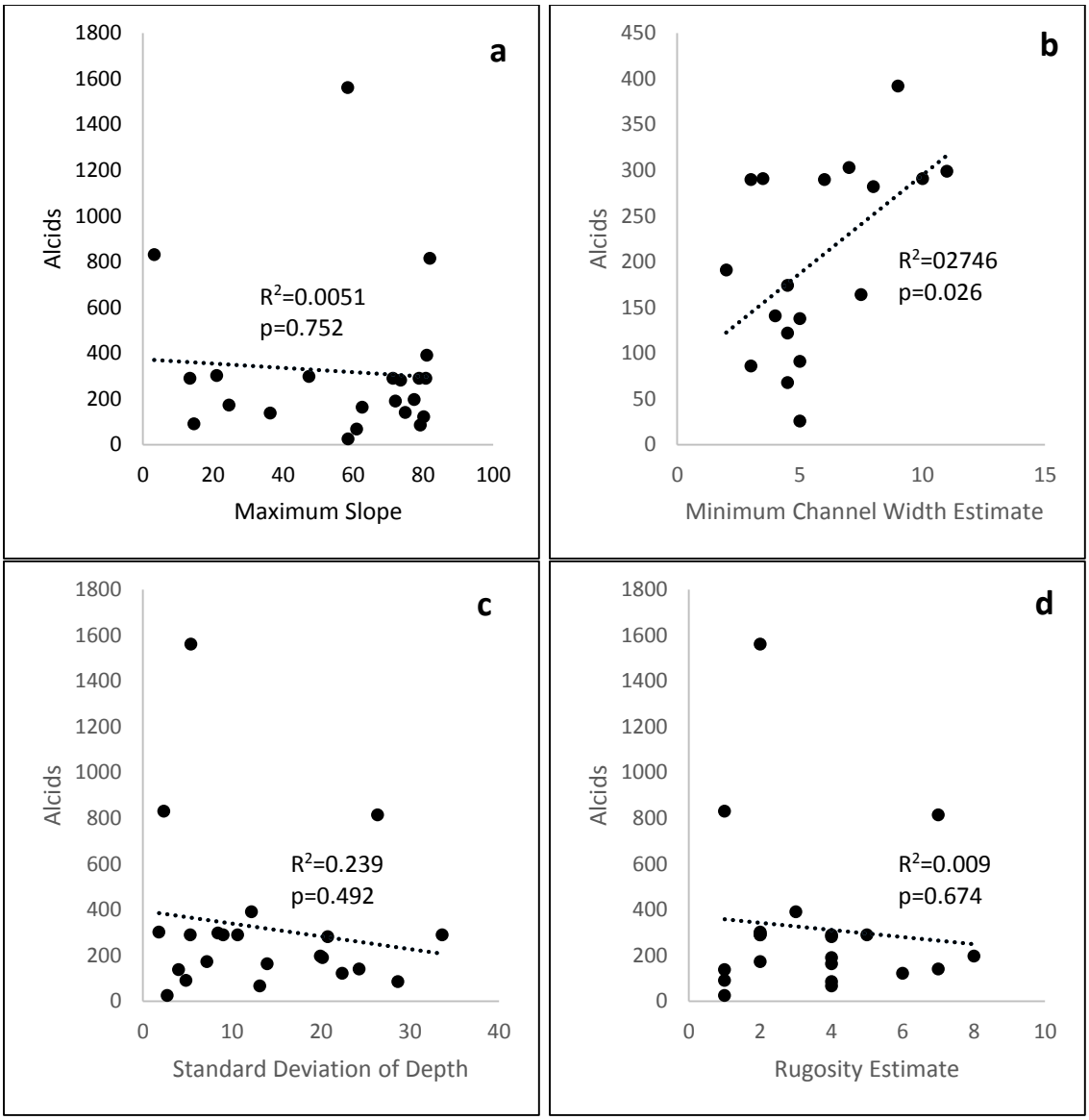

Figure 3. Number of alcids per bin, according to four bathymetric measures of bins: (a) maximum slope, (b) minimum channel width estimate, (c) standard deviation of depth, and (d) rugosity estimate.

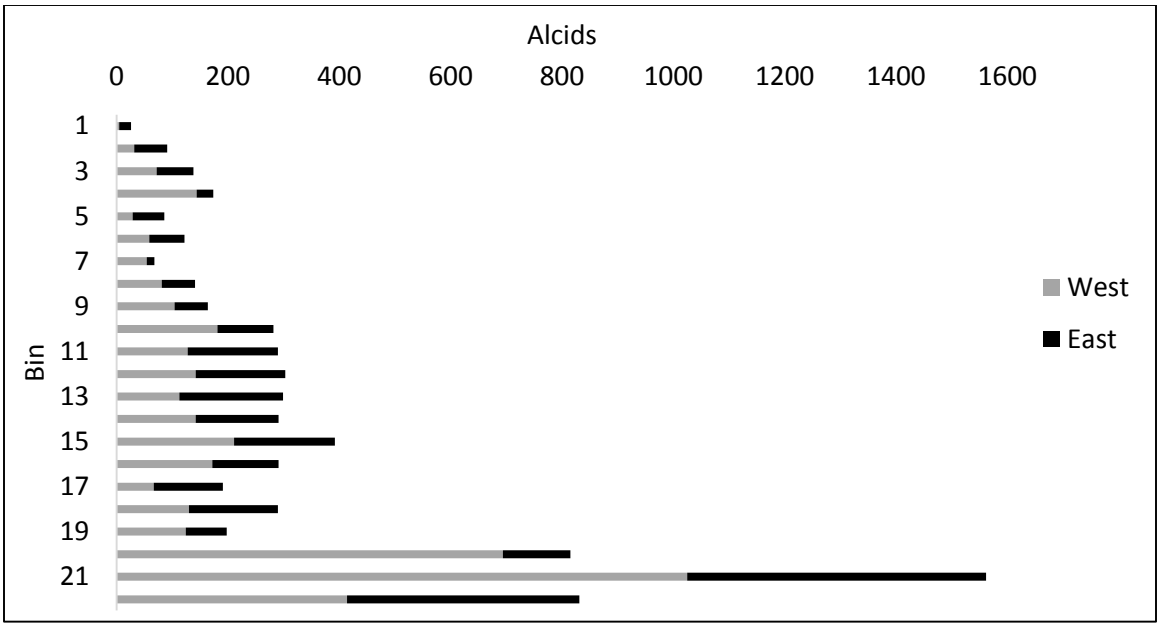

Figure 4. Alcids per bin, divided by west and east sides of bin.

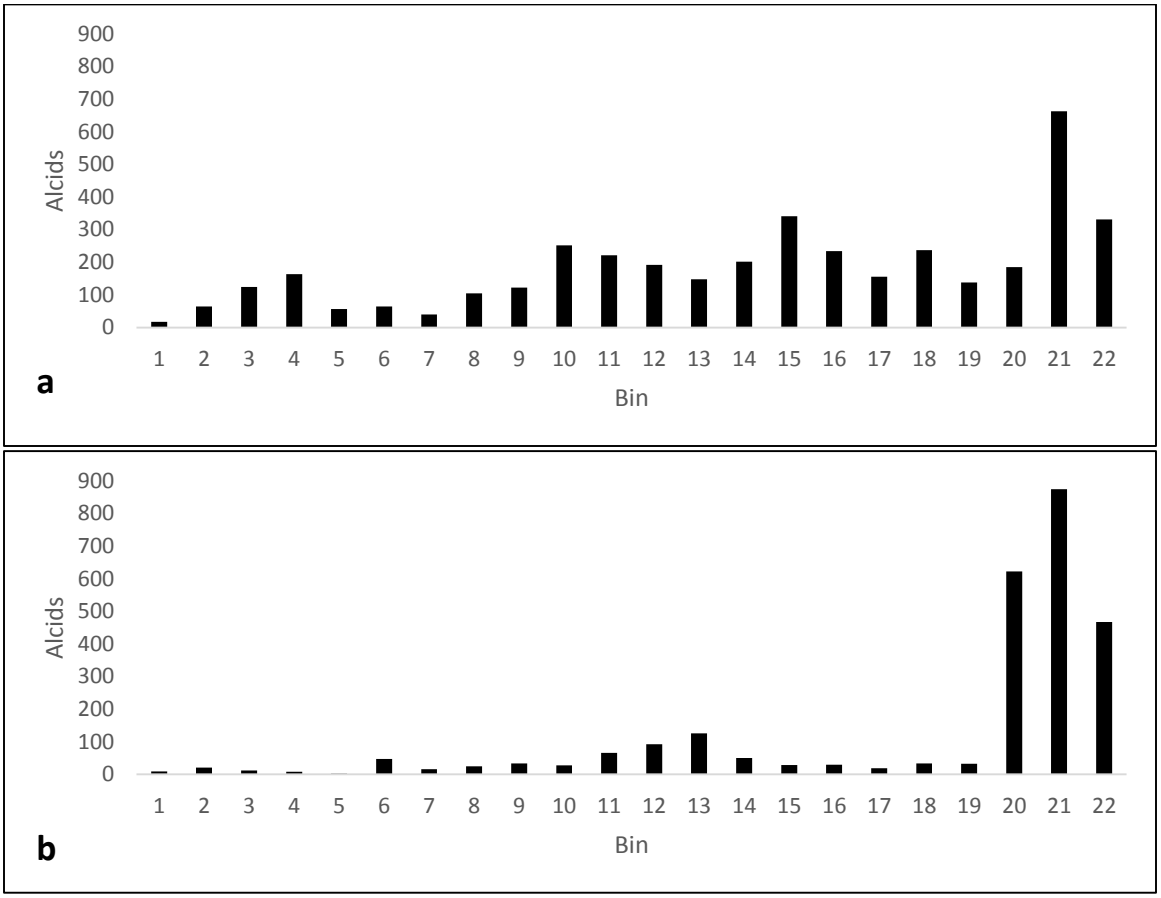

Figure 5. Alcids per bin in transects conducted on (a) flood and (b) ebb tides.

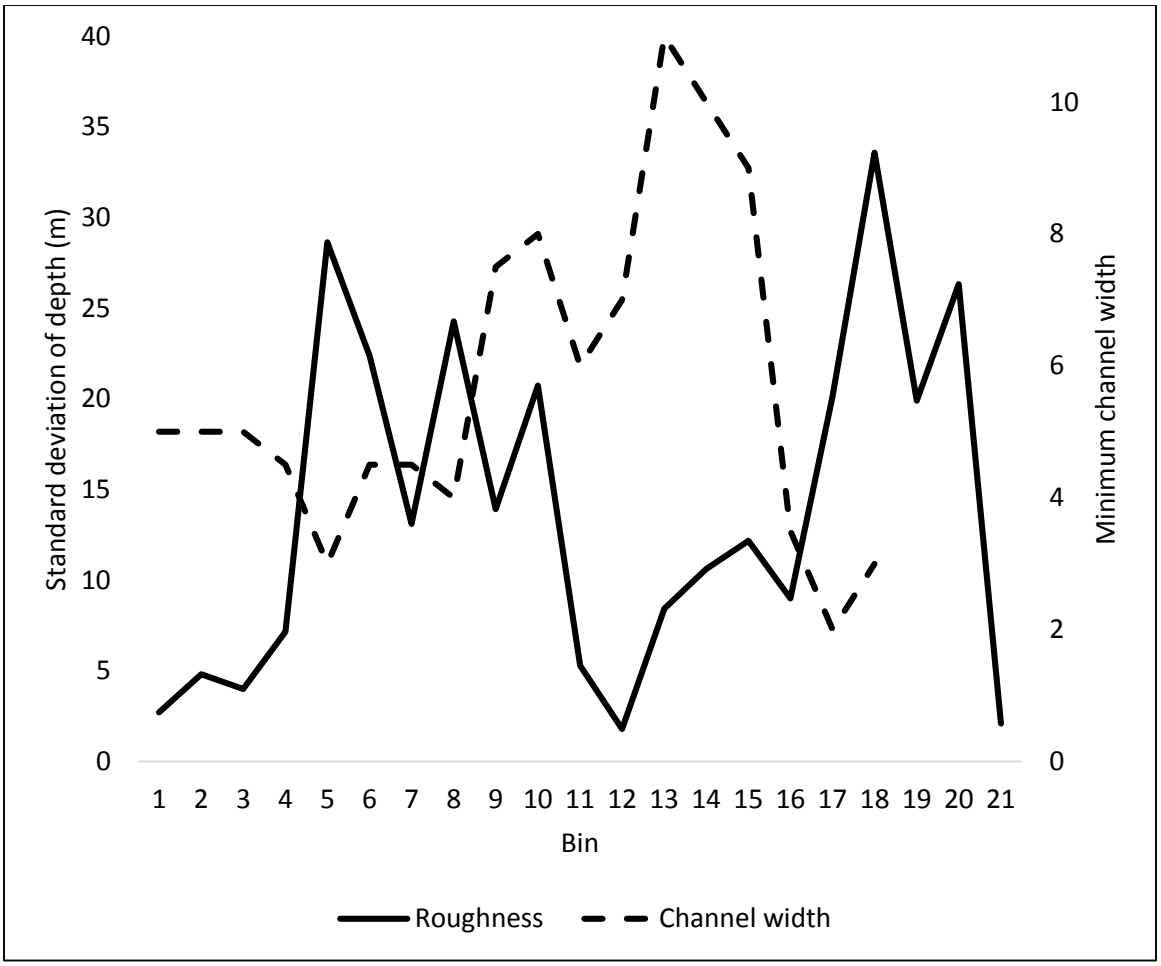

Figure 6. Standard deviation of depth and minimum channel width of bins.

ACKNOWLEDGMENTS

This work would not have been possible without the help of many people, to whom I owe my greatest thanks. To instructors Breck Tyler, Jan Newton, Matt Baker, and RA Derek Smith for the many hours of discussion, thoughtful guidance and constant encouragement at every step of this process. To Dennis Willows, Wolf Krieger, and Phil Green, whose contributions of time and enthusiasm made Centennial cruises not only possible, but delightful. To Gary Greene and John Aschoff for their generosity with their data and willingness to work with me on this uncertain project. To Morgan Eisenlord for her patient and indispensable advice. To Katie Harrington, Andrew Baird, and Carl Wayan-Levine for their cheerful assistance with long hours of small-boat work. To Craig Staude, Alan Cairns, David Duggins, Jeannie Meredith and all the FHL staff for sharing their expertise and for making the labs an amazing place to live and work. Finally, to my fellow PEF apprentices: Alicia Highland, Atinna Gunawan, Hilary Standish, Jen Lopez, Jessi Thompson, Laura Bliss, Rebekka Gould, and Tom Pham. I've learned so much from working with you.